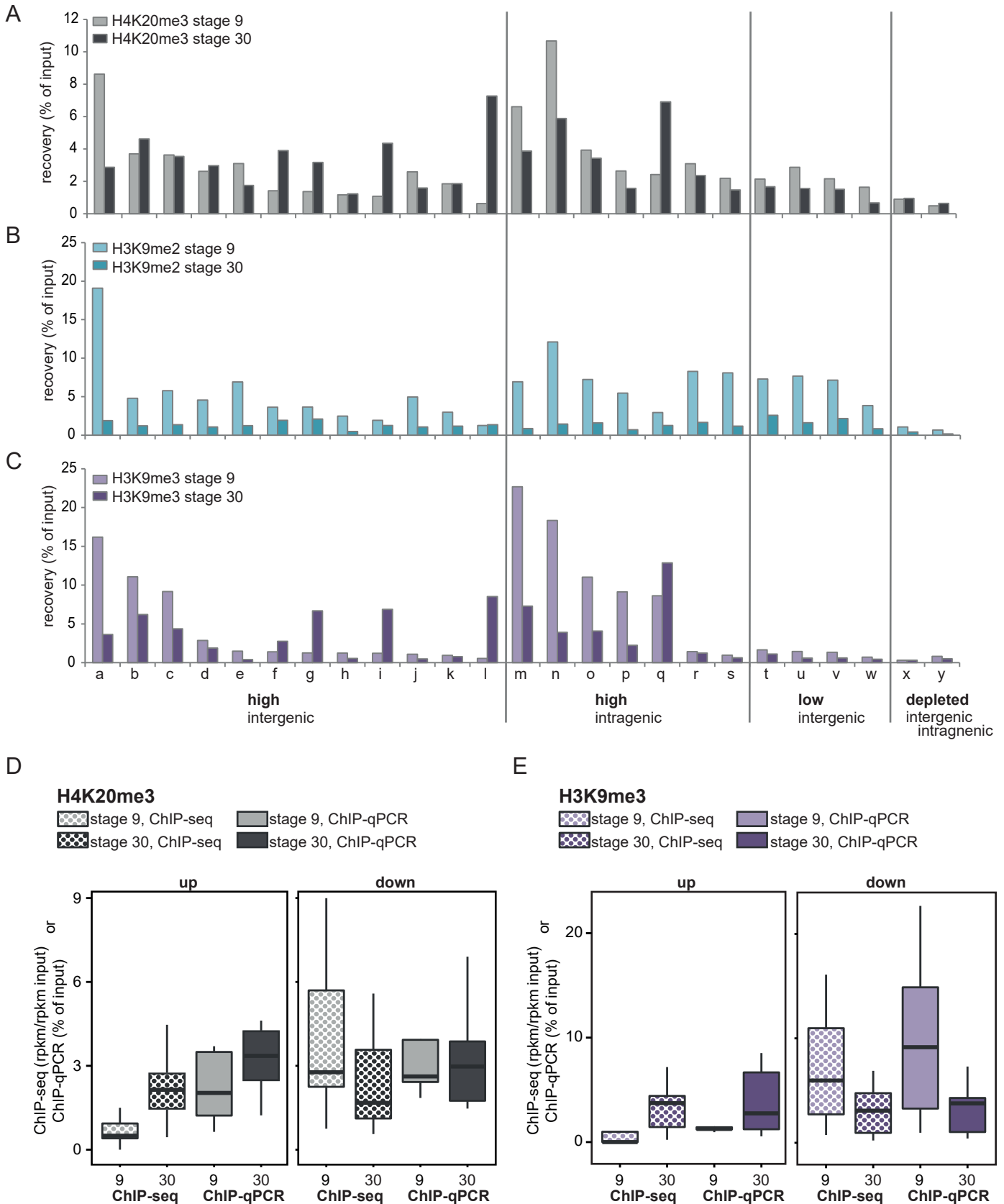


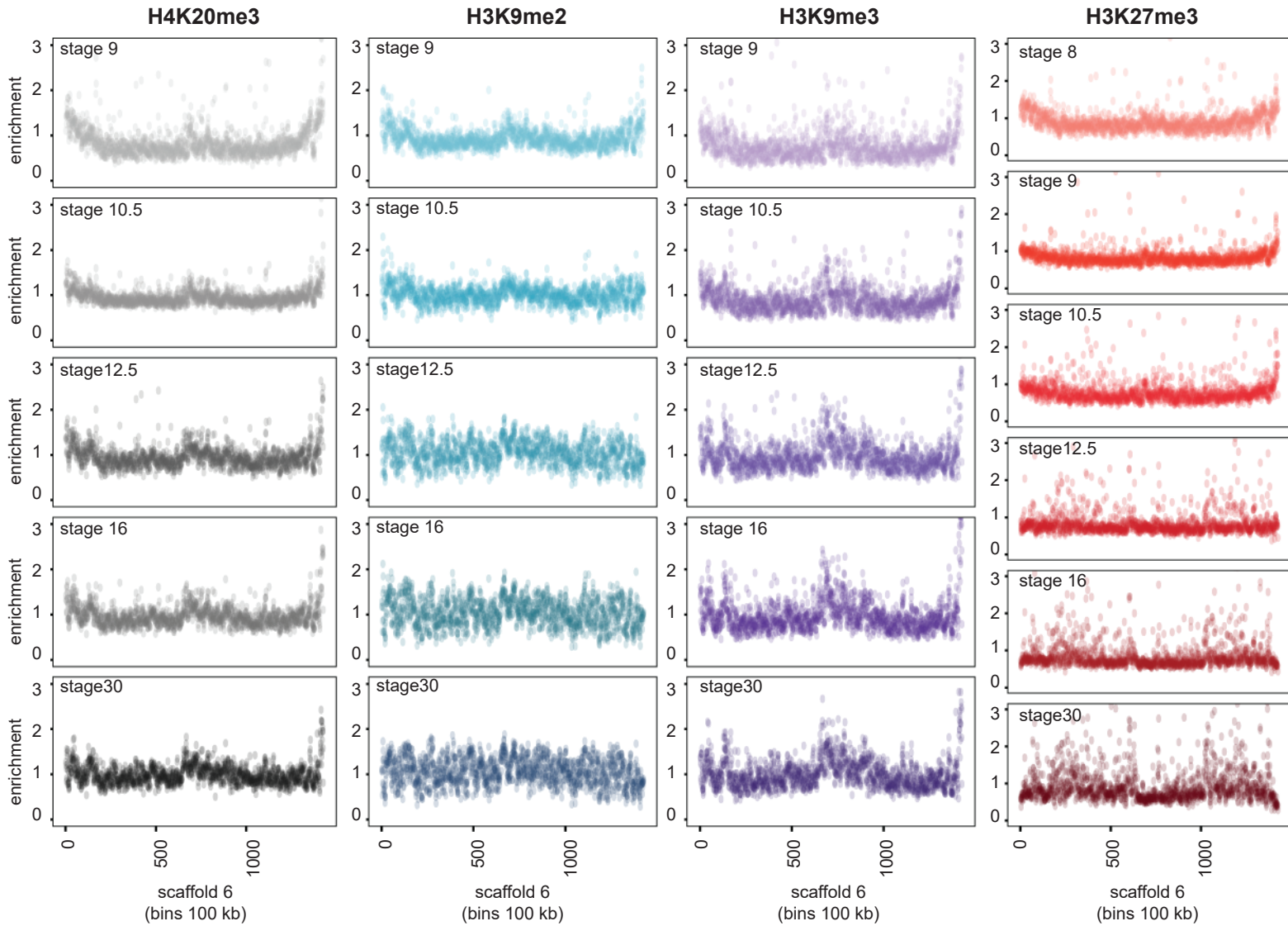
Supplemental figure 1



Supplemental Fig. 1: Comparison of ChIP sequencing and ChIP-qPCR. A, B, C) ChIP-qPCR for H4K20me3, H3K9me2 and H3K9me3 was performed at stage 9 and 30. Primers were designed for inter- and intragenic loci which had high, low, or no coverage in ChIP-seq for H4K20me3 and/or H3K9me3 (as indicated on x-axis). Recovery from input (%) was plotted. D, E) Dynamics of H4K20me3 and H3K9me3 between stage 9 and 30 were compared between ChIP-seq and ChIP-qPCR. Locus 'a' to 's' (panel A, C) were grouped by up- or downregulation according to the ChIP-seq data, after which boxplots were generated. Enrichment over input track was plotted for ChIP-seq and recovery of input was plotted for ChIP-qPCR.

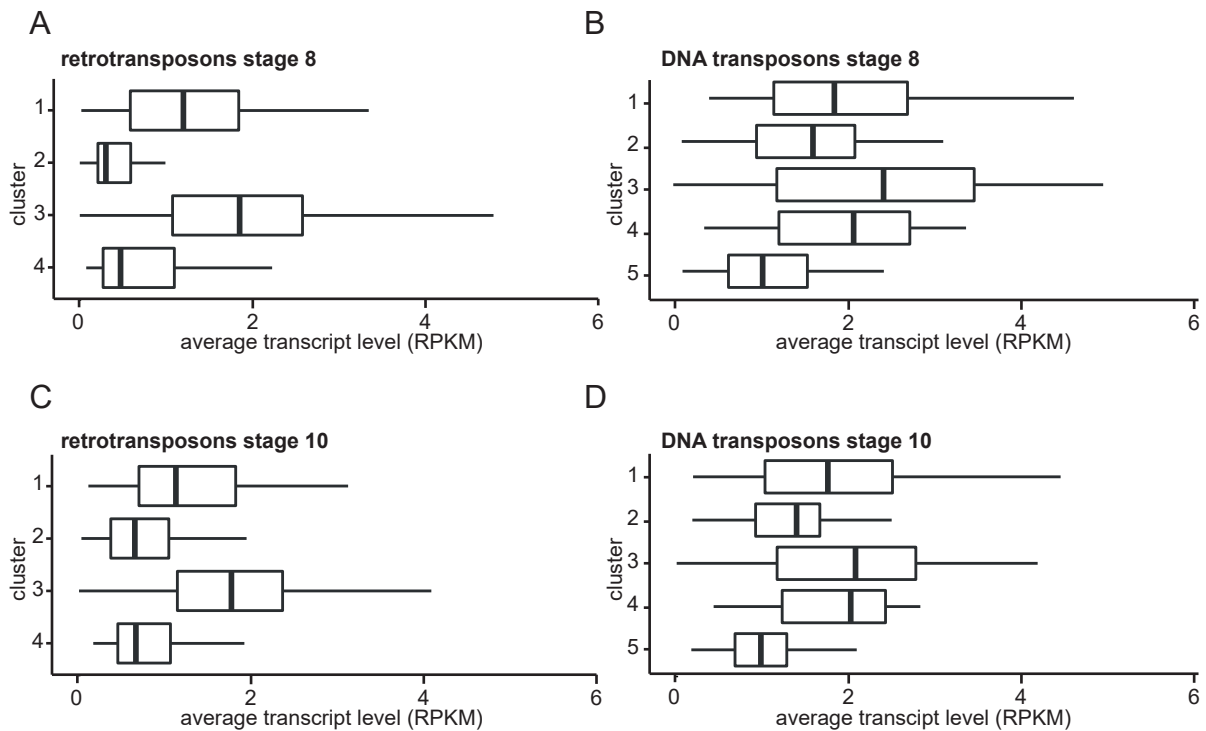
Supplemental figure 2

scaffold 6



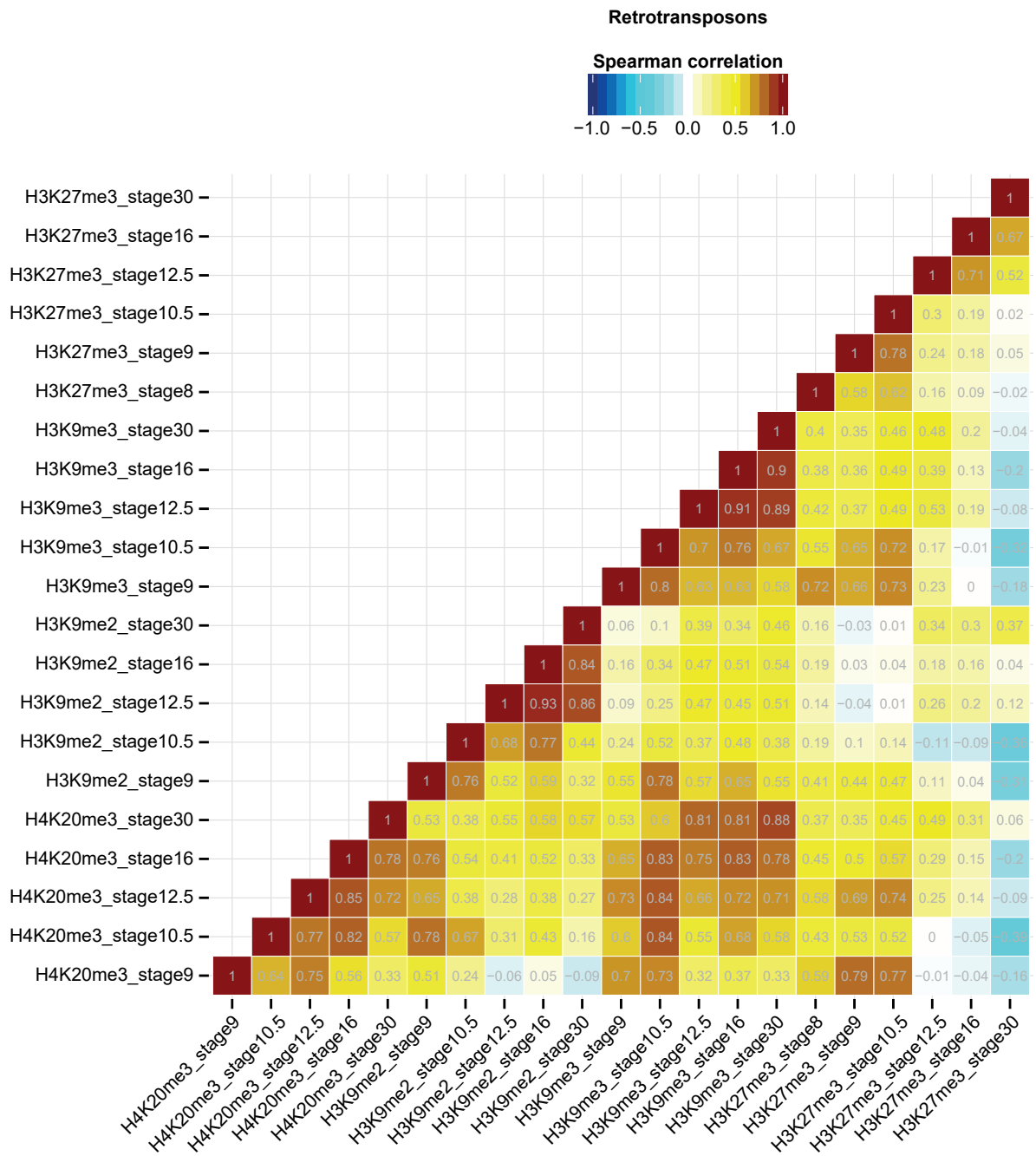
Supplemental Fig. 2: Distribution of heterochromatic histone modifications over scaffold 6. Each scaffold was divided in bins of 100 kb. RPKM of the heterochromatic histone modification was calculated for each bin. Enrichment of H4K20me3, H3K9me2, H3K9me3 and H3K27me3 (left to right) at stage(8,) 9, 10.5, 12.5, 16 and 30 (top to bottom) over the input track was visualized for each bin.

Supplemental figure 3



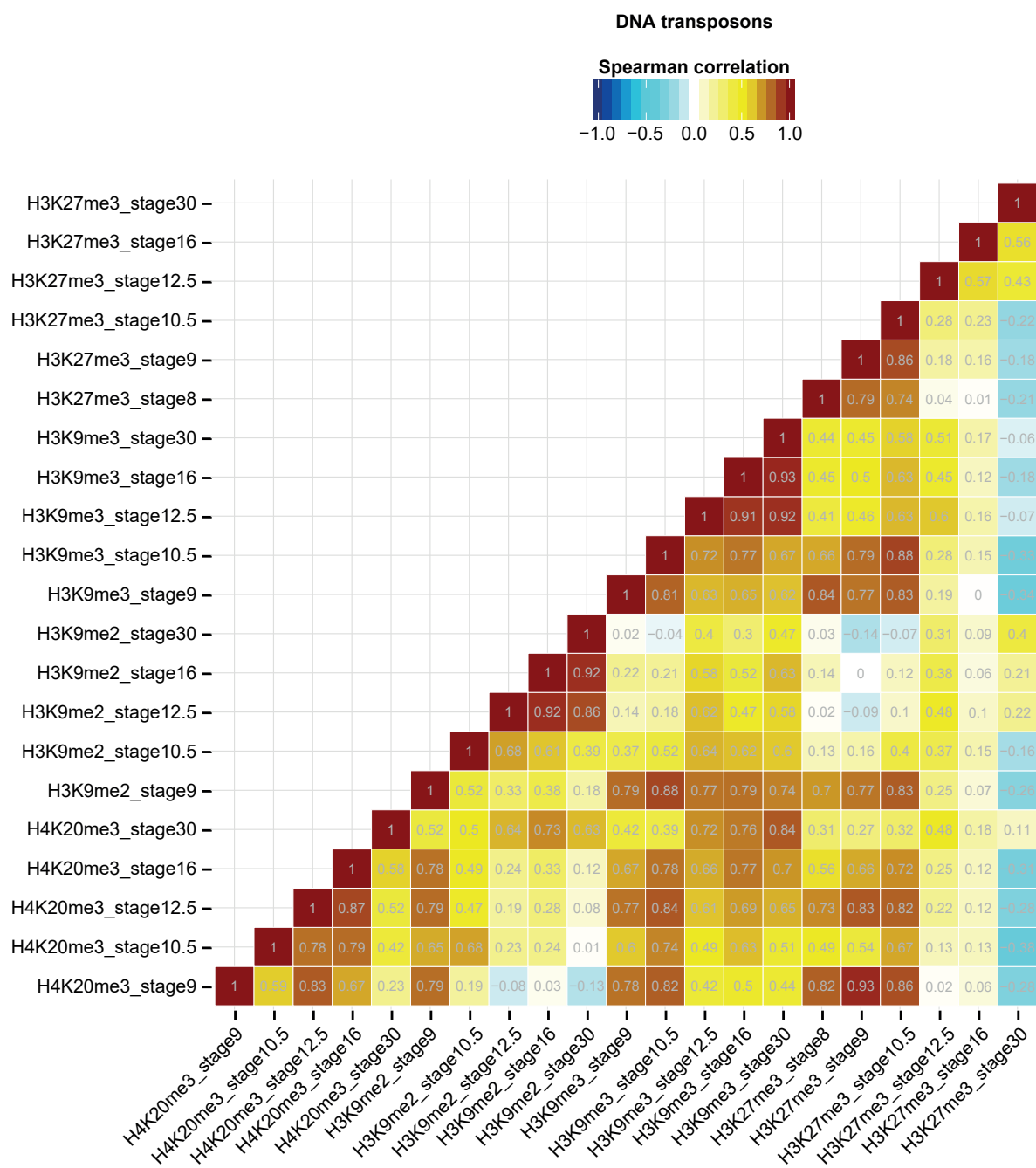
Supplemental Fig. 3: Relatively low transcript levels for transposon clusters with most abundant heterochromatin marking. For each TE subfamily the medium transcript abundance (RPKM) was calculated for embryos in A, B) stage 8 and C, D) stage 10. A, C) Retro- and B, D) DNA transposons were grouped according to clusters as determined in Fig. 2A, B. Average transcript levels for the subfamilies were plotted for each clusters: the left and right hinges correspond to the cluster's 25th and 75th percentiles and the vertical line in between represents the cluster's median RPKM.

Supplemental figure 4



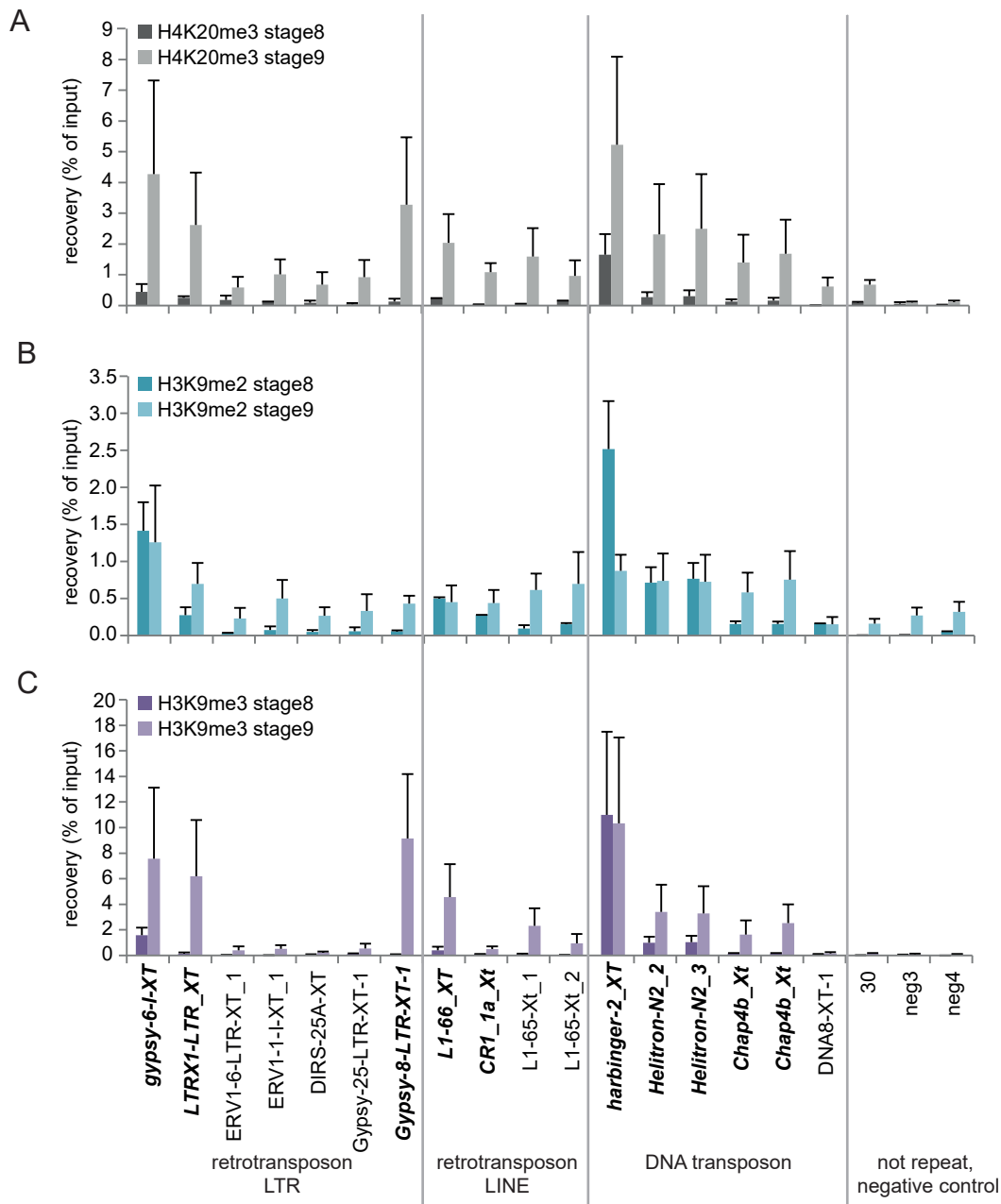
Supplemental Fig. 4: Correlation plot of histone modifications at retrotransposons. The median enrichments of each heterochromatic histone modification for each retrotransposon subfamily were used to calculate spearman correlation, as indicated by color and values.

Supplemental figure 5



Supplemental Fig. 5: Correlation plot of histone modifications at DNA transposons. The median enrichments of each heterochromatic histone modification for each DNA transposon subfamily were used to calculate spearman correlation, as indicated by color and values.

Supplemental figure 6

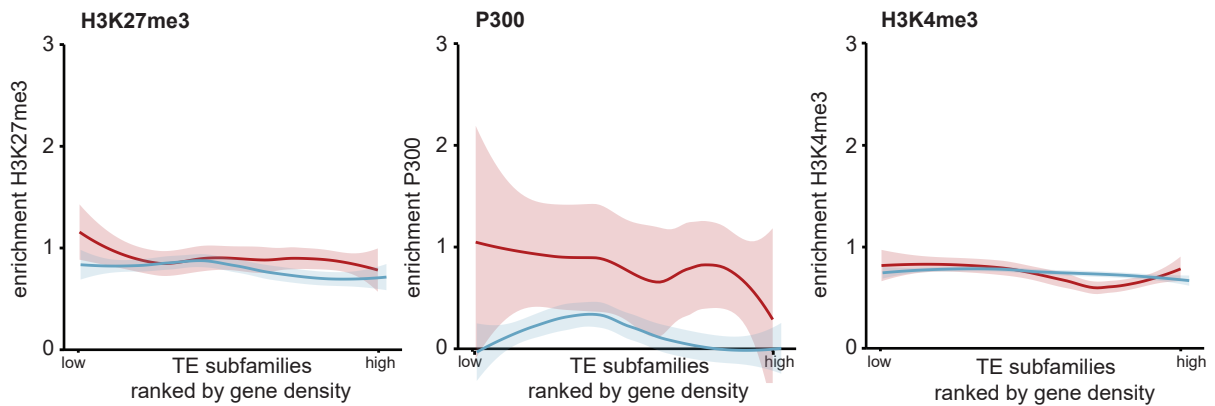


Supplemental Fig. 6: H4K20me3 and H3K9me3 acquired in stage 9. ChIP against A) H4K20me3, B) H3K9me2 and C) H3K9me3 were performed in stage 8 (dark bars) and in stage 9 (light bars). Recovery of input was analyzed by qPCR for various transposon types, as indicated on the x-axis. Transposons written bold+italic are the individual transposons enriched for at least one heterochromatic mark in the stage 9 ChIP-seq data. n=2, average +SEM.

Supplemental figure 7

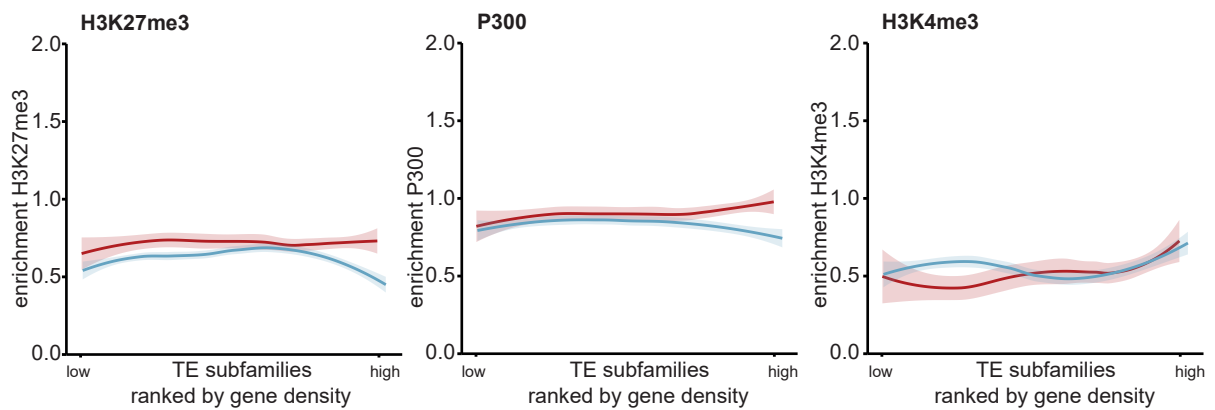
A

stage 9:



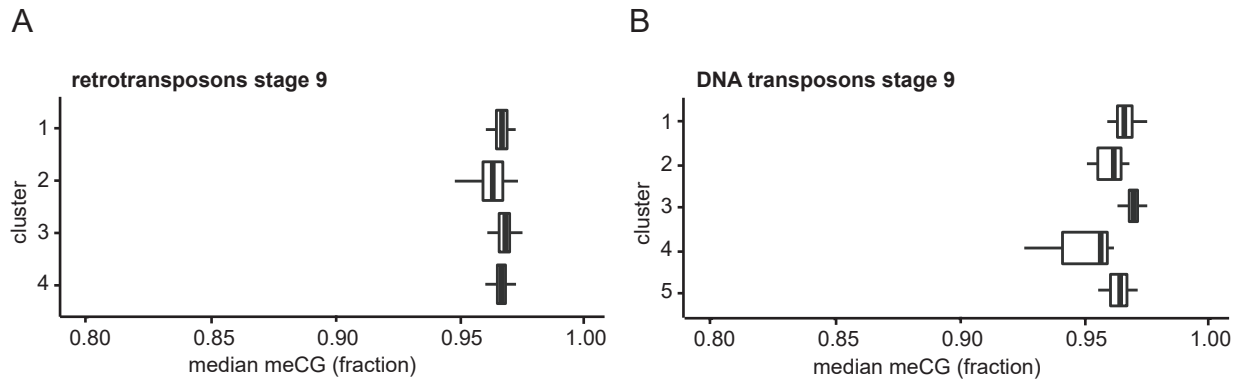
B

stage 30:



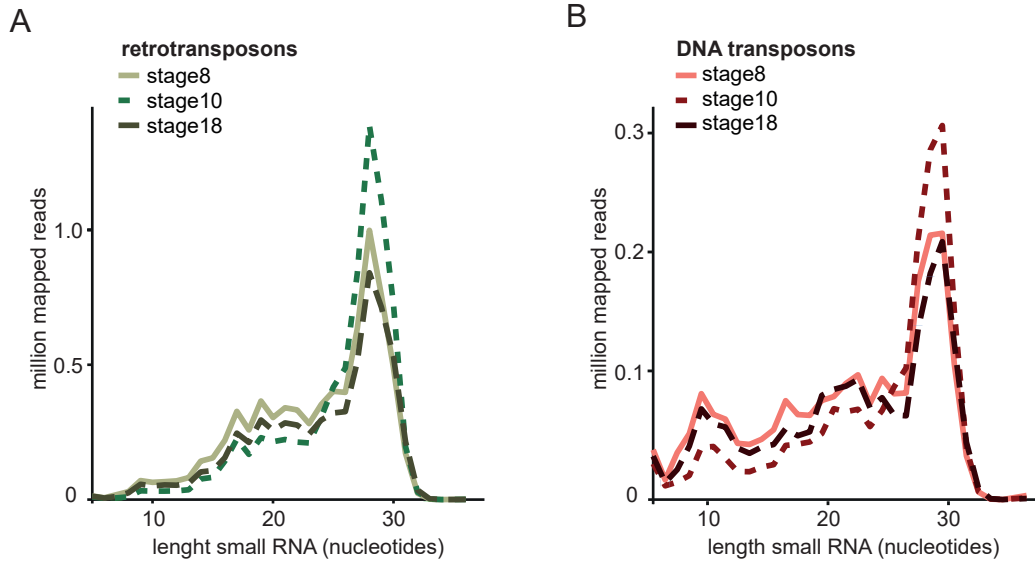
Supplemental Fig. 7: H3K27me3, P300 and H3K4me3 at transposons do not anti-correlate with gene density. For each TE subfamily the median gene density was calculated 500.000 bp up- and downstream of the center of each TE. All TE subfamilies were ranked by gene density and median H4K27me3 (left), P300 (middle) and H3K4me3 (right) enrichments during stage A) 9 and B) 30 were plotted for retro- (blue) and DNA transposon (red) subfamilies. Loess was used as smoothing method, with a 0.95 confidence interval.

Supplemental figure 8



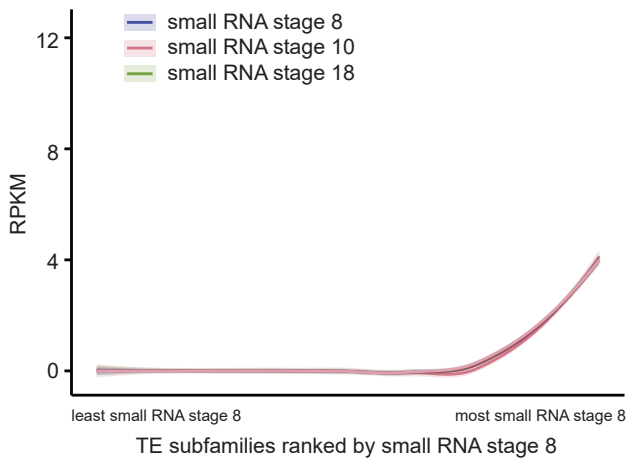
Supplemental Fig. 8: Transposons are hypermethylated during blastula stage. Median methylation fraction ($=\text{meCG}/(\text{meCG}+\text{CG})$) during stage 9 was calculated for each subfamily. meCG fraction was plotted for A) retro- and B) DNA transposon subfamilies grouped according to clusters determined in Fig. 2A, B. The left and right hinges correspond to the 25th and 75th percentiles and the vertical line in between represents the median.

Supplemental figure 9



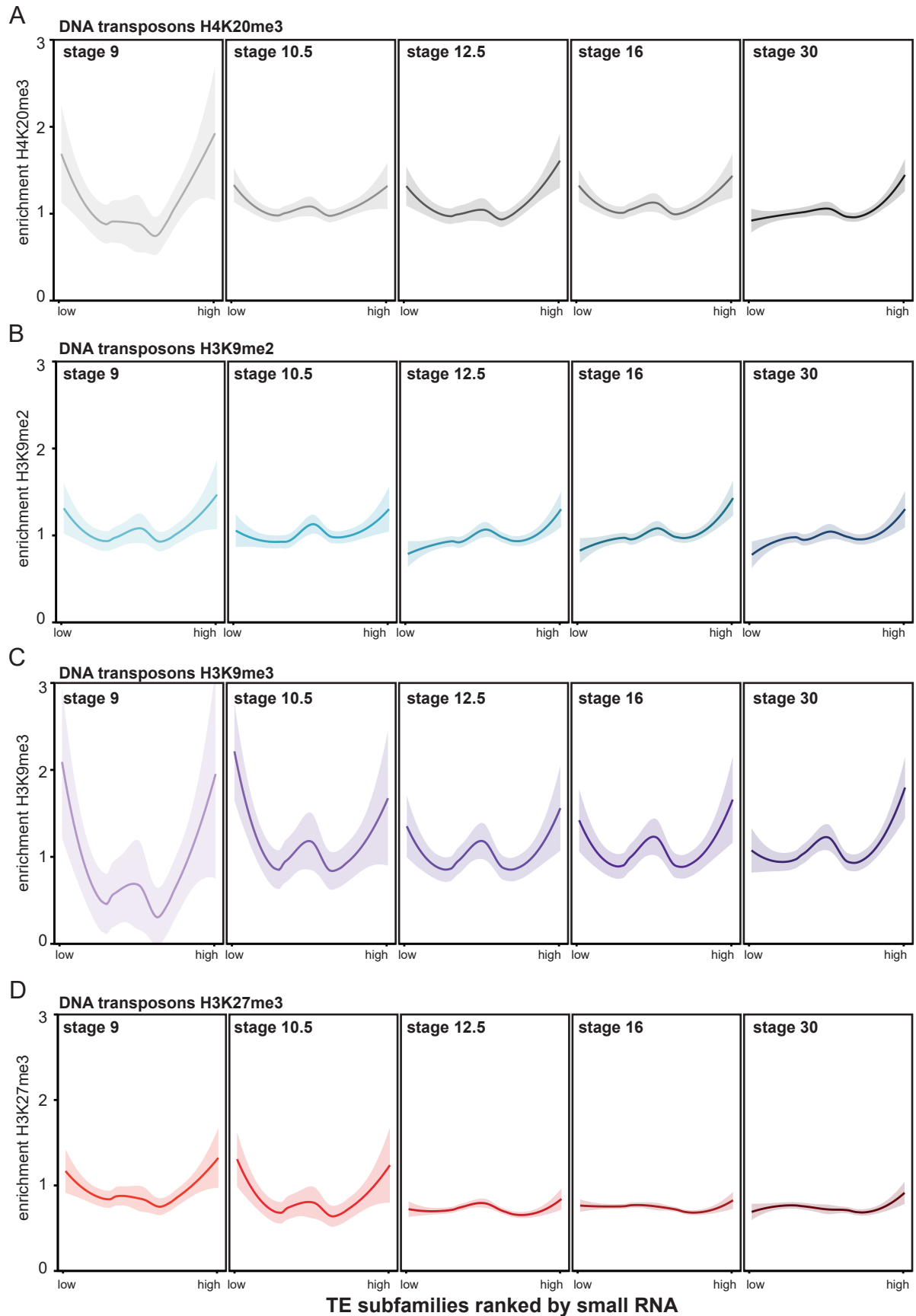
Supplemental Fig. 9: The majority of small RNA mapping to transposons is 28 nucleotides long. Small RNA reads (stage 8, 10 and 18) that aligned to A) retro- and B) DNA transposons were split based on nucleotide length (x-axis) and counted (y-axis).

Supplemental figure 10



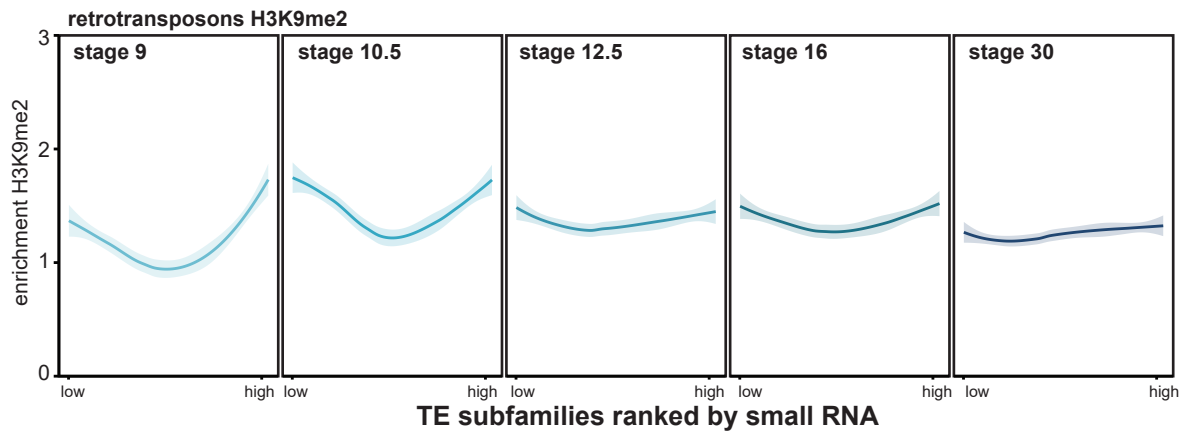
Supplemental Fig.10: The transposons subfamily ranking for small RNA is largely stable during development. Median small RNA levels (RPKM) at stage 8, 10 and 18 were calculated for each TE subfamily. All TE subfamilies were ranked by amount of small RNA at stage 8 and small RNA levels for all three stages were plotted in this order. Loess was used as smoothing method, with a 0.95 confidence interval (line shade).

Supplemental figure 11



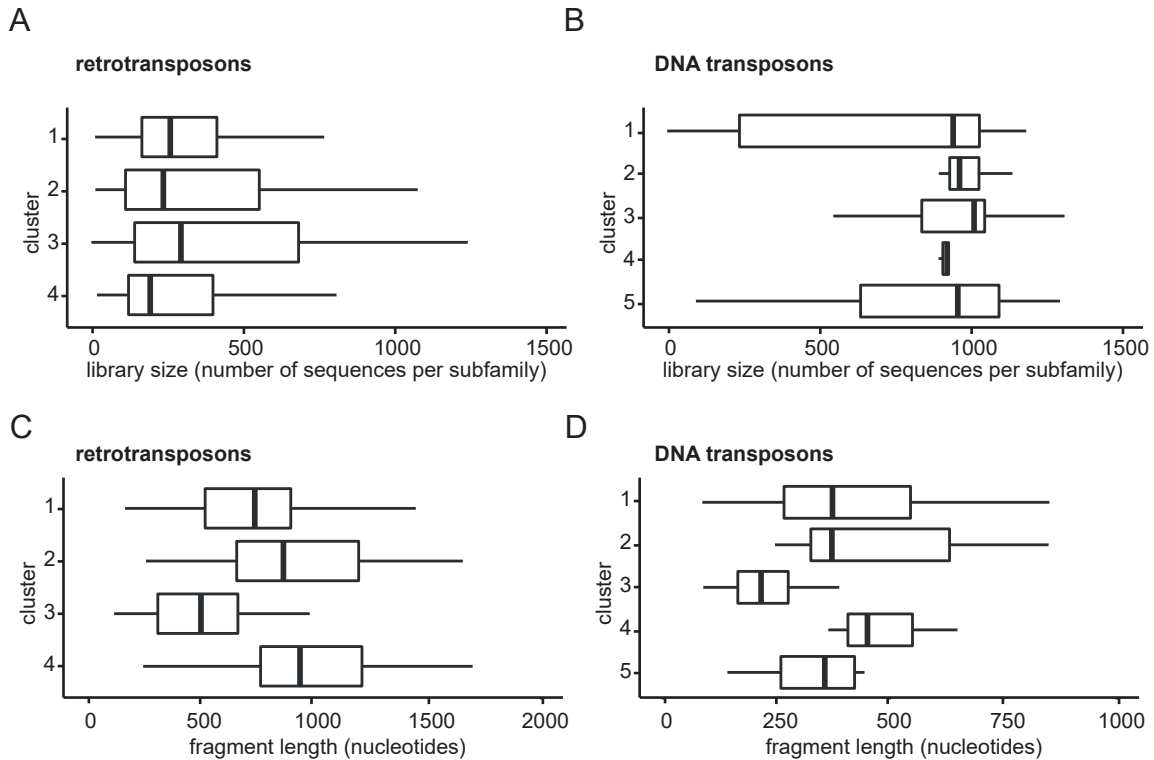
Supplemental Fig. 11: Small RNA does not correlate with heterochromatic histone modifications at DNA transposon subfamilies. All TE subfamilies were ranked by amount of small RNA and in this order median A) H4K20me3, B) H3K9me2, C) H3K9me3 and D) H3K27me3 enrichments were visualized for DNA transposons. Histone marks were plotted for stage 9, 10.5, 12.5, 16 and 30 (left to right). The line was plotted using Loess smoothing method, with a 0.95 confidence interval (line shade).

Supplemental figure 12



Supplemental Fig. 12: Small RNA does not correlate with H3K9me2 at retrotransposons. All TE subfamilies were ranked by amount of small RNA and in this order median H3K9me2 enrichment for each retrotransposon subfamily was visualized. Histone marks were plotted for stage 9, 10.5, 12.5, 16 and 30 (left to right). The line was plotted using Loess smoothing method, with a 0.95 confidence interval (line shade).

Supplemental figure 13



Supplemental Fig. 13: Library sizes and fragment lengths of retro- and DNA transposon clusters. The individual sequences per TE subfamily were counted. These library sizes were plotted for the A) retro- and B) DNA transposon clusters as determined in Fig. 2A, B. The median length of the sequences belonging to each TE subfamily was determined and these median fragment lengths were also plotted for the C) retro- and D) DNA transposon clusters as determined in Fig. 2A, B. The left and right hinges correspond to the 25th and 75th percentiles and the vertical line in between represents the median.